DOI: 10.31393/morphology-journal-2024-30(1)-01 Reports of Morphology, Vol. 30, №1, Pages 5-15

ISSN 1818-1295 eISSN 2616-6194

REPORTS OF MORPHOLOGY

Official Journal of the Scientific Society of Anatomists, Histologists, Embryologists and Topographic Anatomists of Ukraine

journal homepage: https://morphology-journal.com

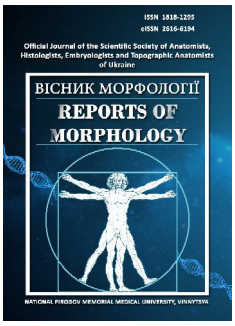

Comparative assessment of tissue response to a mesh implant made of polypropylene modified with carbon nanotubes and silver nanoparticles

Viltsaniuk O. A., Kravchenco V. M., Viltsaniuk O. O., Dereziuk A. V., Sheremeta R. O.
National Pirogov Memorial Medical University, Vinnytsya, Ukraine

ARTICLE INFO
Received: 15 November 2023
Accepted: 03 January 2024

UDC: 616.34-007.43-089:581.41:599.323.4:612.08

CORRESPONDING AUTHOR
e-mail: viltsanyuk@gmail.com
Viltsaniuk O. A.

CONFLICT OF INTEREST
The authors have no conflicts of interest to declare.

FUNDING
Not applicable.

DATA SHARING
Data are available upon reasonable request to corresponding author.

Treatment of abdominal hernias remains one of the most urgent problems of modern surgery. A large number of complications after hernia operations require the development of new types of implants for tissue plastic surgery. The purpose of the study is to carry out an experimental comparative assessment of tissue reaction to the implantation of the developed polypropylene mesh implant modified with carbon nanotubes and silver nanoparticles. Research was conducted on 105 sexually mature laboratory rats in three series of experiments (35 rats each). In the first series, polypropylene mesh implants were implanted in the tissues of the anterior abdominal wall, in the second - polypropylene implants coated with an antiseptic, and in the third - polypropylene implants modified with carbon nanotubes and silver nanoparticles. Animals were removed from the experiment after preliminary anesthesia 3, 5, 7, 14, 21, 30 and 90 days after the operation. The tissues of the abdominal wall were taken together with the implants, histological preparations were made, which were stained with hematoxylin and eosin and according to Van Gieson. We studied the composition and ratio of elements of cell infiltration in tissues with further statistical processing of the obtained data. It was established that during the implantation of mesh edoprostheses, regardless of their type, necrotic changes with reactive inflammation, the presence of inflammatory cell infiltrate, tissue swelling and microcirculation disorders were detected in the tissues 3-5 days after the operation. Under the condition of implantation of the developed mesh, a less pronounced exudative phase of inflammation and an earlier onset of the reparation phase were detected. Depending on the type of implant used, the subsequent reaction differed between the groups of experimental animals, which was evidenced by the regression of inflammatory phenomena in the tissues and the processes of formation of the fibrous capsule around the implants. During the implantation of nanomodified mesh implants by the 7th day of the experiment, the exudative phase of inflammation ended and the formation of a thin connective tissue capsule began, the formation of which was completed by the 21st day of observation, while when the mesh was implanted with polypropylene and polypropylene with an antimicrobial coating, the formation of the capsule lasted up to 30 days. Thus, it was established that the exudative phase of inflammation continues in the tissues around the implantation of classic polypropylene and polypropylene meshes with an antimicrobial coating up to the 14th day of the experiment, and the connective tissue capsule is formed up to the 30th day. At the same time, in the tissues around the mesh implants made of polypropylene modified with carbon nanotubes and silver nanoparticles, the exudative phase of inflammation ended by the 7th day of the experiment. This ensured the intensity of reparative regeneration processes and the separation of the implant from the surrounding tissues by a thin connective tissue capsule for up to 21 days of observation.

Keywords: *polypropylene mesh implants, carbon nanotubes, silver nanoparticles, morphological changes, biological compatibility.*

Introduction

The problems of treating abdominal hernias remain one of the most urgent problems of modern surgery [8, 10, 15].

Today, polypropylene mesh implants are widely used in hernia repair [4, 5, 18, 28]. But the results of the treatment

of this pathology and complications in the postoperative period are not entirely satisfactory, among which purulent-inflammatory ones remain the most severe, lead to recurrence of hernias, require repeated surgical interventions and significantly worsen the quality of life of patients [17, 32]. To eliminate the shortcomings inherent in classic implants, a number of implants with various types of polymer coatings with antimicrobial properties, substances that improve reparative processes and other properties have been developed. But they do not completely satisfy surgeons, since they are used in limited quantities and do not always meet generally accepted requirements.

Therefore, the development of new types of mesh implants of high strength with antimicrobial and other properties remains an urgent problem. The solution of which is possible only by developing implants using materials with new properties.

A modern scientific direction that allows obtaining new materials with given or new properties is nanotechnology, which involves the introduction of nanoparticles into the composition of matrix substances, which give materials new properties [9, 21].

Today, carbon nanotubes and nanoparticles of various metals are widely used as polymer and metal nanofillers [20, 30, 31], which are introduced into matrix substances to obtain new materials or give known materials new properties [6, 7, 11]. The use of nanotechnology made it possible to obtain fundamentally new types of materials with new or specified properties that are widely used in industry, but information on the use of nanocomposite or nanomodified materials in medicine is limited.

Today, polypropylene threads have been created that contain carbon nanotubes and silver nanoparticles, which have high strength and antimicrobial activity and can be used as surgical suture material. On the basis of the obtained threads, which were used as raw materials for the manufacture of mesh implants, we developed a new type of nanocomposite mesh implants with antimicrobial properties. But for the introduction of the developed endoprostheses into clinical practice, it is necessary to study the reaction of tissues to their implantation, which will allow to substantiate their biocompatibility with tissues and develop indications for use in the clinic.

The purpose of the research is to carry out an experimental comparative evaluation of the reaction of tissues to the implantation of the developed polypropylene mesh implant modified with carbon nanotubes and silver nanoparticles.

Material and methods

Experimental studies were performed in compliance with the requirements of international law (the Helsinki Declaration of Human Rights of 1975 and the Vancouver Convention of 1974, 1994 on biomedical experiments), as well as in accordance with the laws and documents on bioethics of Ukraine (protocol of the Bioethics Committee of the National Pirogov Memorial Medical University, Vinnytsya No. 9 dated November 19, 2019).

The experimental part of the work was performed on 105 sexually mature laboratory rats with a body weight of 200 to 250 g in the vivarium of the National Pirogov Memorial Medical University, Vinnytsya, which were maintained in accordance with generally accepted norms. Rats were divided into three series of experiments (35 animals in each series). In the first series of experiments, polypropylene mesh implants were implanted, in the second - polypropylene mesh implants with antimicrobial properties, on which the antiseptic polyhexamethylene guanidine chloride was applied as an antimicrobial agent by spraying. In the third series, developed polypropylene mesh implants made of polypropylene threads were implanted into which carbon nanotubes and silver nanoparticles were introduced at the formation stage.

Operative interventions were performed after premedication with diphenhydramine at the rate of 1.5 mg/kg of body weight and aminazine (0.02 mg/kg), under ketamine anesthesia (by intramuscular injection of ketamine at the rate of 10 mg/kg of rat body weight). After anesthetizing the animals, they were fixed on the table, the operating field was treated with Betadine and alcohol three times, after which a middle laparotomy was performed. The peritoneum, muscles, and aponeurosis of the anterior abdominal wall were sutured, and mesh implants measuring 1.0 x 0.5 cm were placed on the junction line and fixed with separate nodal sutures to the anterior abdominal wall along the junction line, in the first series of experiments, with atraumatic suture material with polypropylene, and in the second - polypropylene suture material covered with an antiseptic, and in the third - polypropylene suture material modified with carbon nanotubes and silver nanoparticles. After that, the skin and subcutaneous tissue were sutured with knotted sutures with the appropriate suture material and the postoperative wound was treated with Betadine. In the postoperative period, the general condition of the animals and the condition of the postoperative wound were monitored. The animals were removed from the experiment by decapitation after preliminary anesthesia with sodium thiopental at the rate of 50 mg/kg of body weight 3, 5, 7, 14, 21, 30 and 90 days after the surgical intervention. In the animals removed from the experiment, body weight was measured, visible skin and mesh implantation sites were evaluated, and tissues of the anterior abdominal wall were excised together with the implants for morphological studies. The tissues taken for the study were fixed in a 10 % solution of neutral formalin, dehydrated, embedded in paraffin, and 3-5 μm thick sections were prepared on a microtome. The prepared histological preparations were stained with hematoxylin-eosin and according to Van Gieson [22]. Microscopy of histological preparations was carried out using an OLIMPUS BX 41 light microscope (certificate of the Ministry of Health of Ukraine on state registration

No. 8120/2008, code 9011800000). Image visualization was performed using the cellSens Entry program (xv Image Processing), morphometry was performed using the Quickphoto micro 3.2 program (license agreement No. 925113924). The composition and ratio of elements of inflammatory cell infiltration was studied using immersion microscopy. In the obtained histological preparations, the density of the cellular infiltrate in the tissues around the implanted meshes, its cellular composition, and the counting of cells of the fibroplastic series (from young fibroblasts to fibrocytes) were evaluated [3].

Identified changes in the examined tissues were documented by micro photography and processed using the Quick PHOTO MICRO 2.3 program.

Statistical data analysis was performed using Statistica 6.4 v12 software, Stat Soft. Inc. and Microsoft Office Excel 2016. Determination of the nature of data distribution was carried out using the Shapiro-Wilk test. Taking into account the assessment of the normality of the data distribution of quantitative parameters, the comparison of groups was carried out using the t-test. For data that had a non-normal distribution, the calculation was performed using the Mann-Whitney (U) test. The marginal level of error of the first kind (α) is accepted at a level of no more than 5 % ($p<0.05$) [1].

Results

The study of morphological changes in the tissues three days after the implantation of endoprostheses showed that there was swelling and inflammatory cell infiltration in the tissues, which was the least when the developed mesh was implanted. In the tissues around the implanted polypropylene mesh, moderately expressed, diffuse, relatively uniform, inflammatory infiltration was determined, which formed a demarcation shaft. The infiltrate was mainly located within the subcutaneous adipose tissue, spread between the contracted elements of the mesh, capturing at the same time the large subcutaneous muscle, the dermis, and the rectus abdominis muscle adjacent to the mesh. Small areas of necrosis, signs of tissue swelling and the formation of micro-abscesses were noted at the level of the grid location. The vessels of the microcirculatory channel were unevenly expanded, full of blood. Focal diapedesis hemorrhages were determined, the destruction of collagen fibers was observed (they were fragmented, in some places in the form of structureless bands and deep masses that unevenly and insufficiently perceived picrofuchsin) and small accumulations of fibrinoid substance were detected.

A similar microscopic picture was found in the location of the polypropylene implant covered with an antiseptic. On histological preparations, areas of necrosis and significant swelling were revealed. Inflammatory cellular infiltration, which formed a demarcation shaft, was located mainly within the subcutaneous fat tissue, not involving the dermis, but spread to the rectus abdominis muscle. A productive reaction in the form of a thin (in 1-3 layers of cells) epithelioid cell wall was observed directly around the mesh elements, and in places, on the contrary, an exudative reaction with the formation of microabscesses.

In the tissues around the implants, there was an expansion of the lumen and a moderate fullness of the vessels of the microcirculatory channel and large accumulations of fibrinoid substance (Fig. 1).

During this period of observation, the tissues around the polypropylene mesh modified with carbon nanotubes and silver nanoparticles showed slight signs of edema, dilated blood vessels, focal diapedesis hemorrhages, and unevenly expressed cellular infiltration.

The infiltrate was mainly located around part of the mesh threads and within the subcutaneous fat tissue, and unlike previous series of experiments, it did not invade the dermis and the rectus abdominis muscle to which the implant was attached. The cellular composition of the infiltrate did not differ from its composition in previous series of experiments and was also represented by neutrophilic

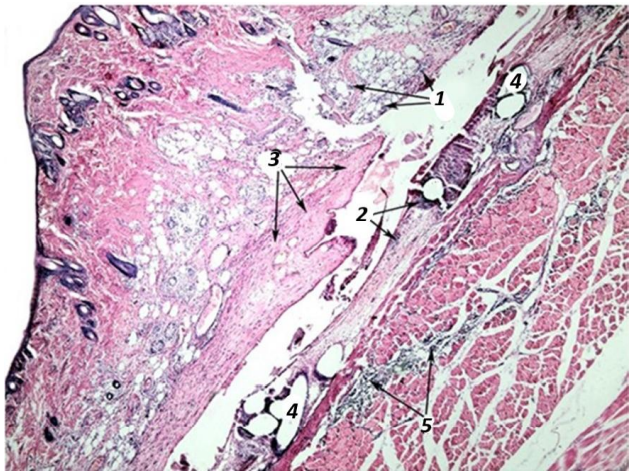

Fig. 1. Inflammatory leukocyte infiltration in the hypodermis (1), in the tissues and rectus abdominis muscle (2, 5), fibrinoid substance (3) around the implanted polypropylene mesh with an antimicrobial coating (4) on the 3rd day of the experiment. Staining with hematoxylin and eosin. x40.

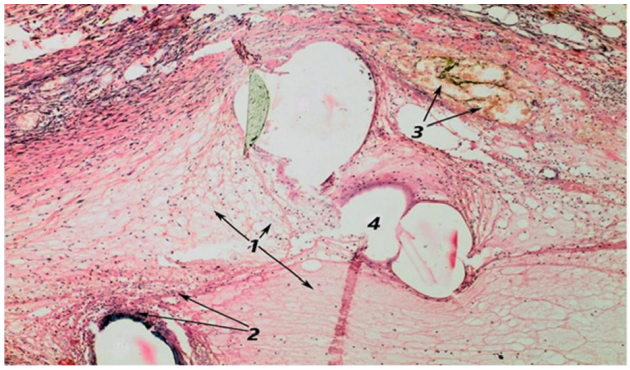

Fig. 2. Tissue swelling (1), inflammatory leukocyte infiltration (2), dilated blood vessels (3) around the implanted polypropylene mesh modified with silver nanoparticles and carbon nanotubes (4) on the 3rd day of the experiment. Staining with hematoxylin and eosin. x100.

leukocytes, plasma cells, lymphocytes and macrophage-monocytic elements. Small areas of fibrinoid substance deposition were found at the level of the mesh location (Fig. 2).

During the morphometric study of changes in cellular composition after 3 days of the experiment, the density of the cellular infiltrate around the implanted meshes was as follows. The infiltrate density around the polypropylene mesh was 812.0±66.5 cells/mm^2. Around the polypropylene mesh coated with an antiseptic, its density was 934.0± 71.0 cells/mm^2 and 622.0±60.3 cells/mm^2 around the developed mesh, which was significantly less ($p<0.005$) than around the meshes implanted in the first and second series of experiments. The study of the composition of the cellular infiltrate showed that the infiltrate in all experiments was dominated by segmented neutrophilic leukocytes, the number of which around the polypropylene mesh was at the level of 714.6±58.6 cells/mm^2, around the polypropylene mesh with an antimicrobial coating - 756.5±57.6 cells/mm^2 and the lowest number of neutrophils of leukocytes ($p<0.05$) was in the composition of the infiltrate around the developed meshes - 485.2±47.0 cells/mm^2. The number of plasma cells in the infiltrate was: around the polypropylene mesh - 18.71±4.03 cells/mm^2, around the polypropylene mesh covered with an antiseptic up to 74.70±5.69 cells/mm^2 and around the designed meshes 62.20±6.05 cells/mm^2; lymphocytes - 32.48±2.60 cells/mm^2 around polypropylene mesh, 56.02±4.30 cells/mm^2 around mesh covered with an antiseptic and 43.51±4.24 cells/mm^2 around developed mesh. Macrophage-monocytic elements were detected around polypropylene meshes in the amount of 16.23± 1.32 cells/mm^2, around meshes covered with antiseptic 46.74±3.52 cells/mm^2 and 31.11±3.00 cells/mm^2 around developed meshes. In the tissues, cells of the fibroblastic series were also detected, which were represented mainly by young fibroblasts, the number of which was significantly higher around the elements of the developed mesh - 209.9±12.3 cells/mm^2, while around the polypropylene meshes their number was at the level of 114.0± 7.6 cells/mm^2 and around of polypropylene nets covered with an antiseptic, cells of the fibroblastic series were found in a small amount - 94.40±5.20 cells/mm^2.

On the seventh day after implantation of polypropylene endoprostheses, inflammatory cell infiltration in tissues became more pronounced. At the same time, the infiltrate was located not only within the subcutaneous adipose tissue and between the structural elements of the mesh, but also spread to the rectus abdominis muscle. Young granulation tissue was found in the tissues in the central parts of the implanted mesh. A granulation shaft of epithelioid cells was located directly around part of the mesh elements, among which there were multinucleated giant foreign body cells of various types (Fig. 3).

At the location of the polypropylene implant covered with an antiseptic, during this period of observation, moderate swelling of the tissues was determined, the mesh itself

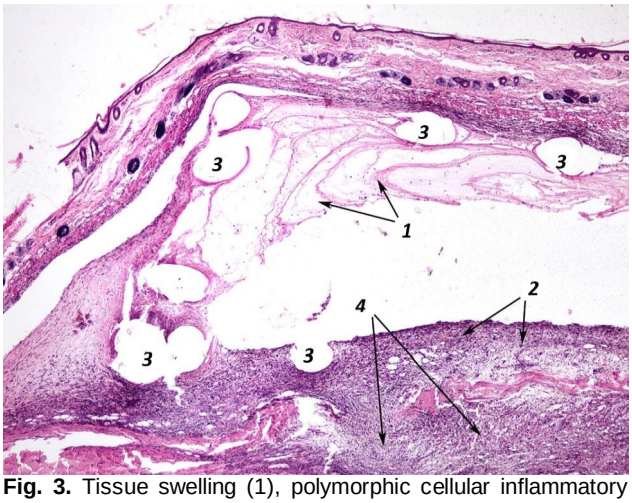

Fig. 3. Tissue swelling (1), polymorphic cellular inflammatory infiltration (2) in tissues (3) and rectus abdominis muscle (4) around the implanted polypropylene mesh on the 7th day of the experiment. Staining with hematoxylin and eosin. x40.

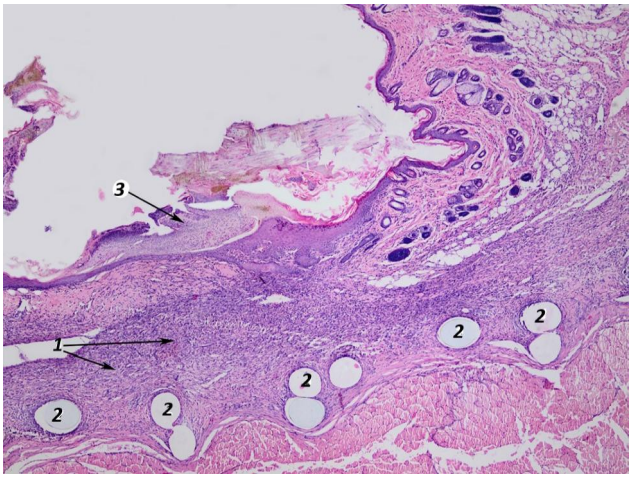

Fig. 4. Granulation tissue with polymorphic cellular inflammatory infiltration (1) in the tissues around the implanted polypropylene mesh covered with an antiseptic (2), scab on the surface of the postoperative wound (3) on the 7th day of the experiment. Staining with hematoxylin and eosin. x40.

had a slightly pronounced deformation. Inflammatory cellular infiltration remained in the tissues, which had a diffuse character. At the same time, its expressiveness has significantly decreased compared to the previous period of observation. Inflammatory infiltration persisted in the hypodermis, in the area of connected tissues, in the area after the surgical wound, and in the form of small foci in the rectus abdominis muscle. Granulation tissue of various degrees of maturity was located around the mesh itself and its individual elements, among which cells of the fibroplastic series and multinucleated giant foreign body cells of various types were determined (Fig. 4).

On the seventh day, there was no tissue swelling around the implanted mesh made of polypropylene modified with carbon nanotubes and silver nanoparticles. Inflammatory cell infiltration became diffuse, its density was significantly

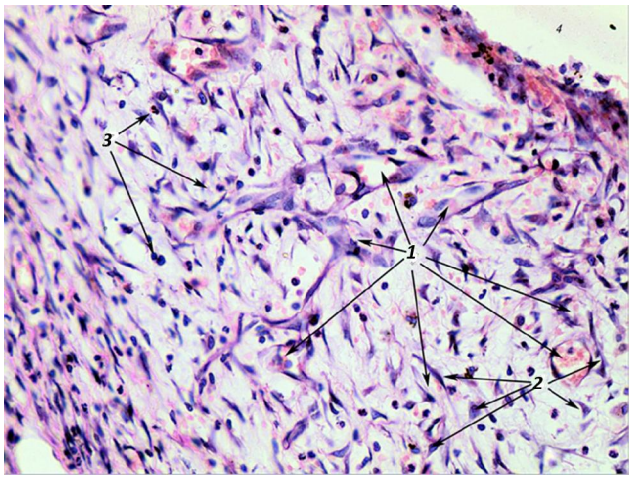

Fig. 5. Vessels of young granulation tissue (1), active fibroblasts (2), eosinophilic granulocytes (3) in the tissues around the implanted polypropylene mesh modified with silver nanoparticles and carbon nanotubes on the 7th day of the experiment. Staining with hematoxylin and eosin. x400.

lower ($p<0.05$) than in the experiments of the comparison groups. The inflammatory infiltrate in the form of cells occupied only the hypodermis, it did not spread to the rectus abdominis muscle. At the same time, abundant masses of fibrinoid substance were deposited at the site of mesh implantation. Granulation tissue of various degrees of maturity with an intercellular matrix and a large number of active fibroblasts was determined around the mesh and its individual elements (Fig. 5).

On the 7th day of observation, the density of the cellular infiltrate around the implanted meshes around the polypropylene meshes increased to 1032±74 cells/mm^2, around the polypropylene mesh with an antimicrobial coating to 810.0±40.1 cells/mm^2, and around the implanted polypropylene mesh modified with carbon nanotubes and silver nanoparticles - 843.0±47.9 cells/mm^2. At the same time, there was a change in the composition of the cells that were found in the infiltrate.

The number of neutrophil leukocytes compared to the previous period of observation decreased significantly ($p<0.05$) and was 608.9±44.0 cells/mm^2 around polypropylene meshes, 354.1±20.1 cells/mm^2 around polypropylene meshes with an antimicrobial coating and 299.7±14.8 cells/mm^2 around developed nets During this period of observation, a significant ($p<0.05$) increase in the number of plasma cells was noted: around polypropylene meshes, their number was 206.4±14.9 cells/mm^2, around polypropylene meshes with an antimicrobial coating - 178.2±8.8 cells/mm^2 and 143.3±8.1 cells/mm^2 around developed grids. A similar pattern was observed with the number of lymphocytes. Thus, the number of lymphocytes in the cellular infiltrate around polypropylene implants was 123.8±8.9 cells/mm^2, around polypropylene meshes with an antimicrobial coating - 129.6±6.4 cells/mm^2, and around engineered meshes - 151.7±8.6 cells/mm^2. A similar picture was observed with macrophage-monocytic elements, the number of which also increased significantly compared to the previous period of observation and amounted to 92.88±6.70 cells/mm^2 around polypropylene meshes, around polypropylene meshes with an antimicrobial coating - 202.5±10.0 cells/mm^2, and around developed meshes - 193.9±11.0 cells/mm^2. The intensification of the phenomena of reparative regeneration processes and the formation of a connective tissue capsule around the implants during this period of observation was evidenced by an increase in the number of fibroplastic cells in the cellular infiltrate around the implants. It should be noted that the number of these cells was different depending on the type of implant. Thus, the number of fibroblastic cells around polypropylene meshes was 2411±162 cells/mm^2, around polypropylene meshes coated with an antiseptic - 2093±121 cells/mm^2, and around developed meshes - 3904±279 cells/mm^2. In addition to the cells of the regenerative row, multinucleated giant foreign body cells were found in the infiltrate around the meshes. The largest number of them was in the tissues around the implanted mesh covered with an antiseptic - 14.02±1.57 cells/mm^2, around polypropylene meshes - 6.021±2.503 cells/mm^2, and the smallest number was found around the developed mesh - 4.011±1.053 cells/mm^2.

On the 14th day of the experiment, inflammatory changes were detected around the elements of the polypropylene mesh in the surrounding tissues, the granulomatous epithelioid cell mass with plasma cells, fibroblasts and multinucleated giant foreign body cells remained and became more pronounced. Fibrous tissue was determined in the area of polypropylene mesh implantation, which was represented by thin bundles and dissociated collagen fibers. Fibrous tissue, along with collagen fibers, contained a significant number of differentiated fibroblasts. At the same time, in the deep sections, between the elements of the mesh, areas of granulation tissue were preserved. Among the collagen fibers, separate areas of dense infiltration by plasma cells and multinucleated giant cells of foreign bodies were determined.

On the 14th day of the experiment, a slight deformation of the polypropylene mesh covered with an antiseptic was determined. Around it, instead of granulation tissue, fibrous tissue was found, represented by thin bundles of mature and immature collagen fibers, and cellular inflammatory infiltration of tissues remained. An unevenly expressed, vascularized granulomatous shaft of epithelioid cells and neutrophilic granulocytes was located around the mesh elements, which also contained fibroblasts, eosinophils, and multinucleated giant cells of foreign bodies. As in the previous series of experiments, areas of dense cellular infiltration and areas of granulation tissue located between mesh elements were found.

In the tissues around the developed meshes, during this period of observation, fibrous tissue, represented by bundles of different thicknesses and dissociated collagen

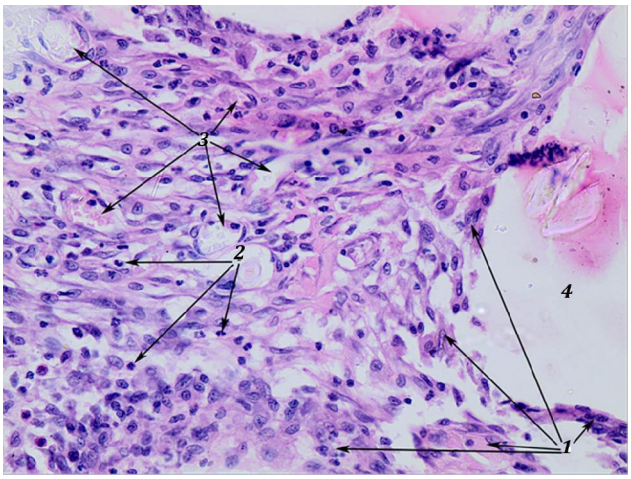

Fig. 6. Granulomatous epithelioid cell shaft (1) with eosinophilic granulocytes (2), microcirculatory vessels (3) in the tissues around the implanted polypropylene mesh modified with silver nanoparticles and carbon nanotubes (4) on the 14th day of the experiment. Staining with hematoxylin and eosin. x400.

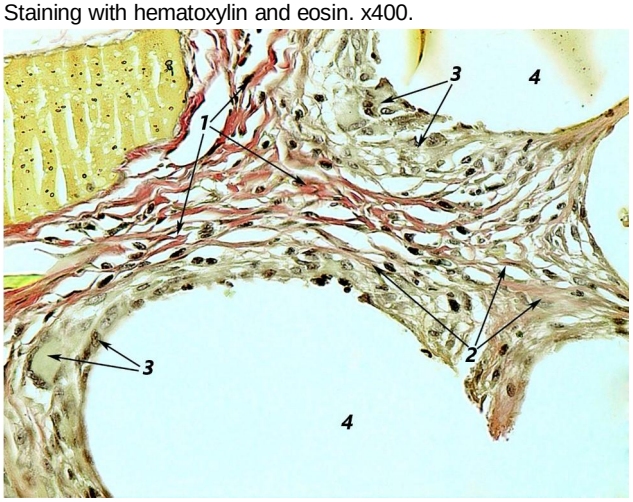

Fig. 7. Mature collagen fibers (1), collagen-producing active fibroblasts (2), granulomatous cell shaft with giant multinucleated cells (3) in the tissues around the implanted polypropylene mesh modified with silver nanoparticles and carbon nanotubes (4) on the 14th day of the experiment. Van Gieson staining. x400.

fibers, was determined on the periphery of the implanted mesh. Collagen bundles and individual fibers of fibrous tissue were ordered, directed parallel to the plane of the mesh, capturing and surrounding its elements. Weakly expressed, scattered inflammatory cellular infiltration was noted in the tissues. Directly around the mesh elements, a thin granulomatous epithelioid cell shaft with the presence of multinucleated giant cells of foreign bodies was preserved (Fig. 6, 7). Inflammatory cell infiltration in the tissues was not determined outside the mesh implantation zone.

The calculation of the composition of cells around the implanted meshes showed that the inflammatory phenomena around the implanted meshes continued to decrease. The density of the cellular infiltrate, during this period of observation, was 413.0±43.5 cells/mm^2 around polypropylene meshes, meshes with an antimicrobial coating - 301.0±22.2 cells/mm^2 and around the developed mesh - 297.0±27.2 cells/mm^2. A decrease in inflammation was also evidenced by a decrease in the number of neutrophil leukocytes in the tissues around the implanted polypropylene mesh to 82.60±8.70 cells/mm^2, around polypropylene meshes with an antimicrobial coating to 24.08±1.82 cells/mm^2, and around the developed mesh - 14.85±1.40 cells/mm^2. Regardless of the type of mesh, during this period of observation, a change in cellular composition was noted, which characterized the predominance of alteration processes over exudation processes and activation of reparative regeneration processes with the formation of a connective tissue capsule around the implants. Thus, the number of plasma cells in the cellular infiltrate around the polypropylene mesh increased to 202.4±21.3 cells/mm^2, to 35.64±3.31 cells/mm^2 around polypropylene meshes with an antimicrobial coating, and to 27.09±2.00 cells/mm^2 around the designed mesh. The number of lymphocytes also increased to 49.56± 5.22 cells/mm^2 around polypropylene mesh, 154.4± 14.1 cells/mm^2 around polypropylene mesh with antimicrobial coating, and 90.32±6.73 cells/mm^2 around designed meshes. The number of macrophage-monocytic elements also increased to 78.47±8.26 cells/mm^2 around the polypropylene mesh, to 92.07±8.45 cells/mm^2 around the polypropylene meshes with an antimicrobial coating, and around the designed mesh to 159.5±11.8 cells/mm^2. Also, the number of cells of the fibroblastic series increased in the tissues around the implanted meshes, the number of which in the infiltrate around the polypropylene meshes was 1852±85 cells/mm^2, around the meshes coated with an antiseptic - 1608±111 cells/mm^2, and around the designed meshes - 2552±138 cells/mm^2. The number of multinucleated giant cells of foreign bodies also increased.

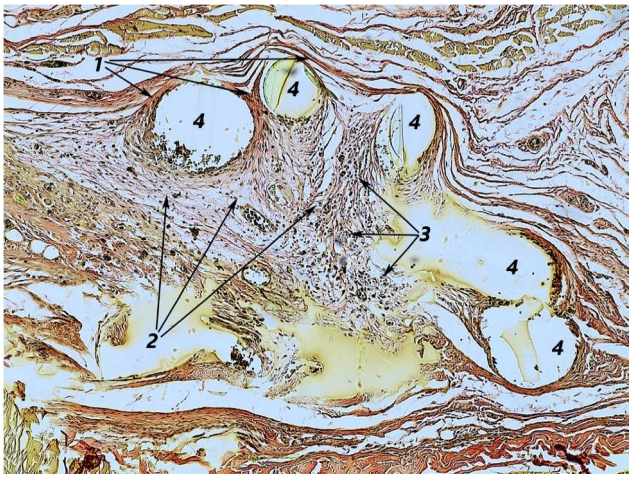

Fig. 8. Areas of mature (1) and immature (2) connective tissue in the fibrous capsule with foci of inflammatory cell infiltration (3) around the implanted polypropylene mesh (4) on the 21st day of the experiment. Van Gieson staining. x100.

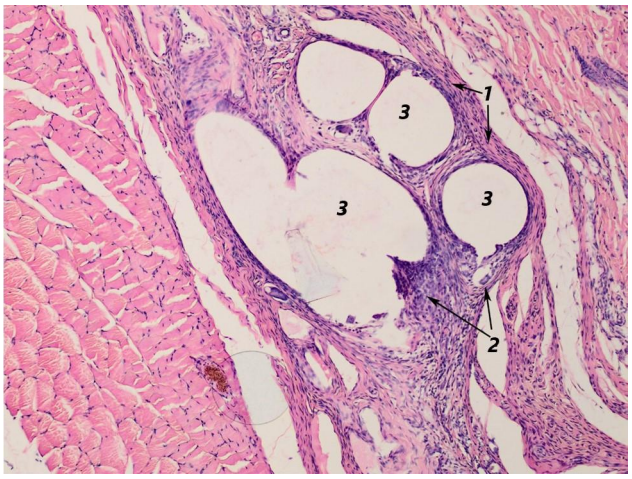

Fig. 9. Connective tissue capsule (1) with foci of inflammatory cell infiltration (2) in the tissues around the implanted polypropylene mesh covered with an antiseptic (3) on the 21st day of the experiment. Staining with hematoxylin and eosin. x100.

In the tissues around the polypropylene mesh up to 7.004±2.750 cells/mm^2, around the meshes with antimicrobial coating - 12.04±2.60 cells/mm^2 and up to 9.027±3.410 cells/mm^2 around the designed mesh.

On the 21st day of the experiment, fibrous tissue of heterogeneous structure and maturity was determined in the area of polypropylene mesh implantation. Along the surface of the grid, the fibrous tissue was represented by a thin layer of densely arranged collagen fibers oriented parallel to the plane of the grid. At the same time, the latter simultaneously penetrated between the mesh elements and incompletely covered them. Between the mesh cells, fibrous tissue was formed by immature thin bundles of collagen fibers. Tissues were unevenly infiltrated with cellular elements. The granulomatous epithelioid cell shaft around the mesh elements, which contained fibroblasts and single multinucleated giant cells of foreign bodies, remained, but became less pronounced (Fig. 8).

On the 21st day of observation, in the area of implantation of a polypropylene mesh covered with an antiseptic, fibrous tissue of a heterogeneous degree of maturity was determined on the surface of the mesh: mature collagen fibers partially enveloped the mesh elements themselves. Along with this, mainly between the mesh elements, areas of fibrous tissue formed by loose thin bundles of immature collagen fibers were determined. In the fibrous tissue, unevenly expressed inflammatory cell infiltration took place. A thin granulomatous, epithelioid-cell shaft, which was preserved around the mesh elements, with individual multinucleated giant cells of foreign bodies was found along the periphery of the mesh in separate places (Fig. 9).

Whereas in the zone of implantation of the nanocomposite mesh, mature fibrous tissue was determined. On the surface of the mesh and around its threads, fibrous tissue was represented by bundles of thickened mature, mostly compactly arranged, collagen fibers. Inflammatory cell infiltration at the mesh implantation site was absent. Single multinucleated giant foreign body cells were found in the tissues directly adjacent to the meshes. Inflammatory phenomena and structural disorders in the tissues beyond the location of the mesh were not detected, which indicated the completion of the processes of formation of the connective tissue capsule around the implanted mesh (Fig. 10).

During the morphometric examination during this period of observation, a slight cellular infiltrate was detected around the meshes, the density of which was 194.0± 12.8 cells/mm^2 around the polypropylene meshes, 206.0±11.5 cells/mm^2 around the polypropylene meshes with an antimicrobial coating, and 173.0±11.8 cells/mm^2 around the developed mesh. Neutrophil leukocytes in the composition of the infiltrate were in small numbers: around the polypropylene nets, their number was 3.461± 0.240 cells/mm^2, around the polypropylene nets with an antimicrobial coating - 2.063±0.127 cells/mm^2, and around the developed net, neutrophil leukocytes were found in the form of single cells. The number of plasma cells also decreased. Their number around polypropylene meshes was 13.84±0.94 cells/mm^2, around polypropylene meshes with an antimicrobial coating - 8.247±0.462 cells/mm^2, and plasma cells were found around the developed mesh in the form of single cells. The number of lymphocytes in the infiltrate remained elevated: around polypropylene meshes up to 76.12±5.19 cells/mm^2, around polypropylene meshes with an antimicrobial coating - 76.22±4.20 cells/mm^2, and around the developed meshes their number was significantly reduced in comparison with control experiments and the previous observation period up to 3.882±0.265 cells/mm^2. However, the number of macrophage-monocytic elements in the cellular infiltrate was not significantly different from the previous period of observation and amounted to 79.58±5.43 cells/mm^2 around polypropylene meshes, 119.5±6.7 cells/mm^2 around

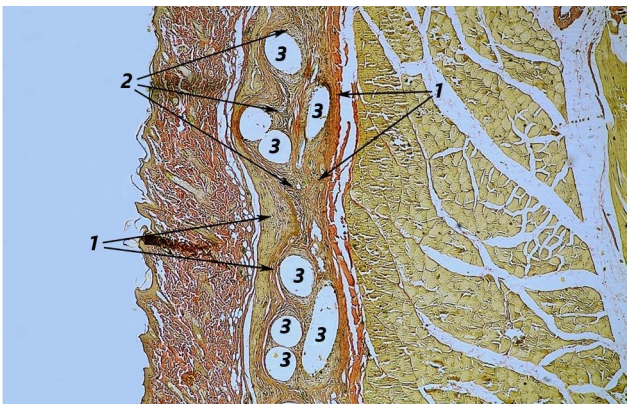

Fig. 10. Fibrous capsule with ordered bundles of collagen fibers (1), granulomatous cellular reaction (2), around the tissues around the implanted polypropylene mesh modified with silver nanoparticles and carbon nanotubes (3) on the 21st day of the experiment. Van Gieson staining. x40.

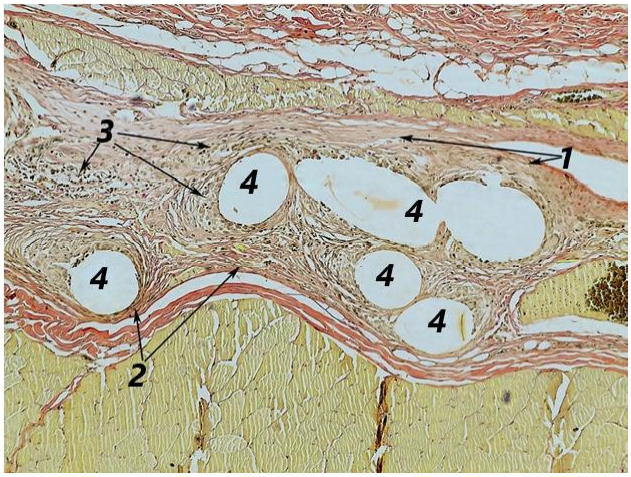

Fig. 11. Areas of immature (1) and mature with ordered bundles of collagen fibers (2) fibrous capsule, granulomatous cellular reaction with an admixture of granulocytes (3) in the tissues around the implanted (4) polypropylene mesh with an antimicrobial coating on the 30th day of the experiment. Van Gieson staining. x100.

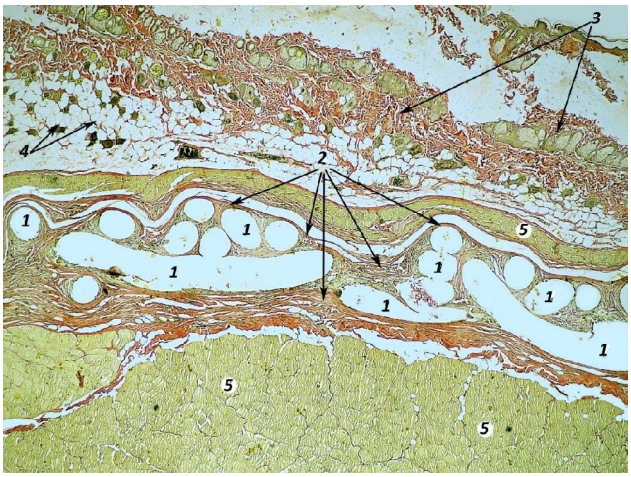

Fig. 12. Implanted polypropylene mesh modified with silver nanoparticles and carbon nanotubes (1), fibrous capsule (2), preserved structure of skin (3), hypodermis (4) and muscles of the anterior abdominal wall (5) on the 90th day of the experiment. Van Gieson staining. x40.

polypropylene meshes with an antimicrobial coating and 190.1±12.6 cells/mm^2 around developed nets During this period of observation, the bulk of the cells in the cellular infiltrate consisted of fibroplastic cells. Thus, their number was 1207±71 cells/mm^2 around polypropylene nets, 1593±100 cells/mm^2 around polypropylene nets with an antimicrobial coating, and 943.0±68.7 cells/mm^2 around developed nets. In addition, the number of foreign body multinucleated giant cells increased: 12.05±5.42 cells/mm^2 around polypropylene mesh, 8.002±3.165 cells/mm^2 around polypropylene meshes with antimicrobial coating, and 7.002±3.235 cells/mm^2 around developed mesh.

On the 30th day, a well-formed capsule of fibrous tissue was found around the implanted polypropylene mesh, represented by uniformly densely arranged bundles of collagen (picrinophilic) fibers oriented along the mesh, covering its individual elements and abdominal muscles in a sleeve-like fashion. Fibrous areas of fibrous tissue sclerosis were determined between the mesh elements. A small number of differentiated fibroblasts were found on the periphery of areas of sclerosis. An uneven epithelioid-cellular granulation shaft with the presence of multinucleated giant cells of foreign bodies and fibroblasts was also preserved around the mesh elements. The structure of the intact dermis and underlying muscle was not altered.

Around the nets with an antimicrobial coating, the histological picture, similar to the previous term, was mostly preserved for a day. A capsule was located around the implanted mesh and its elements, formed by bundles of collagen fibers of various degrees of maturity, associated with collagen fibers of the aponeurosis of the rectus abdominis muscle and the perimysium of the large subcutaneous muscle. An uneven shaft of epithelioid cells with multinucleated giant cells of foreign bodies and active fibroblasts was located around the mesh elements (Fig. 11).

On the 30th day, the fibrous tissue around the implanted developed mesh, the mesh modified with silver nanoparticles and carbon nanotubes, contained bundles of collagen fibers homogeneous in structure and maturity. The latter were located along the plane of the grid and around its elements, forming a clear fibrous capsule intimately connected with the connective tissue formations of the muscles. Inflammatory cell infiltration in the surrounding tissues was not determined. The normal histological structure of the surrounding tissues was also preserved, and the restoration of the spatial structure of the implanted mesh itself was noted.

On the 30th day, a slight cellular infiltrate was detected around the polypropylene implants and around the polypropylene mesh with an antimicrobial coating. The density of the infiltrate was 97.00±6.67 cells/mm^2 around polypropylene meshes and 111.0±14.1 cells/mm^2 around polypropylene meshes with an antimicrobial coating. Whereas no foci of infiltration were detected in the tissues around the developed meshes.

On the 90th day, the processes of formation of the fibrous capsule around the implants were completed and the implants were separated from the surrounding tissues (Fig. 12). During histological examination, foci of inflammatory infiltration and pathological changes were not detected. The cellular composition in the tissues around the implants did not differ from its composition in the tissues before the operation.

Discussion

According to the literature, morphological changes in the tissues around mesh implants in the early days after surgery are characterized by the presence of inflammatory processes with alteration phenomena followed by a transition to reparative processes aimed at delimiting the

implants from the surrounding tissues by a fibrous capsule [2, 13, 23, 25, 26, 29].

The analysis of the obtained data of our research made it possible to establish that during the implantation of mesh endoprostheses in the tissues of the anterior abdominal wall of rats, regardless of their species, in the first days after the operation, the same changes were detected, which are associated with the body's reaction to traumatic damage due to surgical trauma. Intraoperative damage to the tissues of the abdominal wall in experimental animals on the 3-5th day after surgery was manifested by necrotic changes with reactive inflammation, which was evidenced by the presence of an inflammatory infiltrate dominated by neutrophilic leukocytes, tissue infiltration by cellular elements, tissue swelling and marked microcirculation disorders. At the same time, the maximum manifestations of alteration phenomena were observed during the implantation of a classic polypropylene mesh and a polypropylene mesh covered with an antiseptic, and the minimum during the implantation of a developed mesh modified with carbon nanotubes and silver nanoparticles, where a less pronounced exudative phase of inflammation and an earlier onset of the repair phase were detected. But this reaction differed between groups of experimental animals depending on the type of implant used, as evidenced by the regression of inflammatory phenomena in the tissues around the implants and the processes and terms of the formation of the fibrous capsule around the meshes. During the implantation of nanocomposite mesh implants, by the 7th day of the experiment, the exudative phase of inflammation ended and the formation of a thin connective tissue capsule began. The connective tissue capsule around the developed implants was fully formed on the 21st day of the experiment, while when implanting a classic polypropylene mesh and polypropylene with an antimicrobial coating, the formation of the capsule around the implants lasted until the 30th day of the experiment.

According to many researchers [12, 19, 24, 27], surgical trauma and the presence of an implant in the tissues lead to the occurrence of an inflammatory process, which prevents the delimitation of the implant, and contributes to the occurrence of postoperative complications. Long periods of alteration processes around implanted mesh endoprostheses lead to the development of complications in the early postoperative period. At the same time, long periods of reparative processes aimed at the formation of a connective tissue capsule around implants lead to the formation of a predominantly immature, rough, thick fibrous capsule, which in turn leads to the emergence of so-called late postoperative complications, which worsen the quality of life of patients, contribute to the recurrence of hernias and require repeated surgical interventions [7, 14, 16].

A comparative morphometric and morphological analysis of the reaction of the tissues of the anterior abdominal wall in rats to the implantation of the developed mesh showed that the reaction of the tissues to the developed mesh implant is less pronounced than to the polypropylene mesh and the polypropylene implant coated with an antiseptic and indicates the high biocompatibility of the developed mesh implants and the possibility of their use for surgical treatment of abdominal hernias, which will prevent the occurrence of both early and late postoperative complications.

The data we obtained showed a high biocompatibility of the developed implant with the tissues of experimental animals, which requires further study in the clinic during surgical treatment of abdominal hernias.

Conclusions

1. During the implantation of classic meshes made of polypropylene and polypropylene with an antimicrobial coating, the exudative phase of inflammation in the tissues around the implants was detected up to 14 days of observation, and the formation of a connective tissue capsule around the implants lasted up to 30 days of observation.

2. The exudative phase of inflammation in the tissues around the mesh implants made of polypropylene modified with carbon nanotubes and silver nanoparticles was completed by the 7th day of the experiment, which ensured a greater intensity of the reparative regeneration processes and the separation of the implant from the surrounding tissues by a thin connective tissue capsule up to the 21st day of observation.

References

[1] Altman, D. G. (1990). *Practical statistics for medical research.* CRC press. ISBN 978-0-412-27630-9. doi: 10.1201/9780429258589

[2] Ávila, O. R., Parizzi, N. G., Souza, A. P. M., Botini, D. S., Alves, J. Y., & Almeida, S. H. M. (2016). Histological response to platelet-rich plasma added to polypropylene mesh implemented in rabbits. *International braz j urol*, 42(5), 993-998. doi: 10.1590/S1677-5538.IBJU.2015.0319

[3] Avtandilov, H. H. (1990). *Медицинская морфометрия [Medical morphometry].* M.: Медицина=M.: Medicine.

[4] Babiy, I. V., Vlasov, V. V., Pidmurniak, O. O., & Hurnitskyi, A. E. (2019). Результати хірургічного лікування пахвинної грижі за методикою IL LICHTENSTEIN з використанням різних типів імплантатів [Results of surgical treatment of inguinal hernia using the method of IL LICHTENSTEIN using different types of implants]. *Клінічна анатомія та оперативна хірургія=Clinical anatomy and operative surgery,* 18(1), 57-61. doi: 10.24061/1727-0847.18.1.2019.9

[5] Basile, F., Biondi, A., & Donati, M. (2013). Surgical approach to abdominal wall defects: history and new trends. *International journal of surgery,* 11(1), S20-S23. doi: 10.1016/S1743-9191(13)60008-4

[6] Bhandari, V., Jose, S., Badanayak, P., Sankaran, A., & Anandan, V. (2022). Antimicrobial finishing of metals, metal oxides, and metal composites on textiles: a systematic review. *Industrial & Engineering Chemistry Research,* 61(1), 86-101. doi: 10.1021/acs.iecr.1c04203

[7] Fakoori, E., & Karami, H. (2018). Preparation and characterization

of ZnO-PP nanocomposite fibers and non-woven fabrics. *The Journal of The Textile Institute,* 109(9), 1152-1158. doi: 10.1080/00405000.2017.1417681

[8] Gherghinescu, M. C., Copotoiu, C., Lazar, A. E., Popa, D., Mogoanta, S. S., & Molnar, C. (2017). Continuous local analgesia is effective in postoperative pain treatment after medium and large incisional hernia repair. *Hernia,* 21, 677-685. doi: 10.1007/s10029-017-1625-8

[9] Hassan, T., Salam, A., Khan, A., Khan, S. U., Khanzada, H., Wasim, M., ... & Kim, I. S. (2021). Functional nanocomposites and their potential applications: A review. *Journal of Polymer Research,* 28, 1-22. doi: 10.1007/s10965-021-02408-1

[10] International guidelines for groin hernia management (2018). *Hernia,* 22(1), 1-165. doi: 10.1007/s10029-017-1668-x

[11] Jin, K., Eyer, S., Dean, W., Kitto, D., Bates, F. S., & Ellison, C. J. (2019). Bimodal nanofiber and microfiber nonwovens by melt-blowing immiscible ternary polymer blends. *Industrial & Engineering Chemistry Research,* 59(12), 5238-5246. doi: 10.1021/acs.iecr.9b04887

[12] Kallinowski, F., Fortelny, R. H., Köckerling, F., Mayer, F., Morales-Conde, S., & Sandblom, G. (2022). *Editorial: mesh complications in hernia surgery.* Front Surg 9: 841672. doi: 10.3389/fsurg.2022.841672

[13] Kelly, M., Macdougall, K., Olabisi, O., & McGuire, N. (2017). In vivo response to polypropylene following implantation in animal models: a review of biocompatibility. *International urogynecology journal,* 28, 171-180. doi: 10.1007/s00192-016-3029-1

[14] Köckerling, F., Hoffmann, H., Adolf, D., Weyhe, D., Reinpold, W., Koch, A., & Kirchhoff, P. (2020). Female sex as independent risk factor for chronic pain following elective incisional hernia repair: registry-based, propensity score-matched comparison. *Hernia,* 24, 567-576. doi: 10.1007/s10029-019-02089-2

[15] Köckerling, F., & Simons, M. P. (2018). Current concepts of inguinal hernia repair. *Visceral medicine,* 34(2), 145-150. doi: 10.1159/000487278

[16] Kroese, L. F., Kleinrensink, G. J., Lange, J. F., Gillion, J. F., Ain, J. F., Beck, M., ... & Zaranis, C. (2018). External validation of the European hernia society classification for postoperative complications after incisional hernia repair: a cohort study of 2,191 patients. *Journal of the American College of Surgeons,* 226(3), 223-229. doi: 10.1016/j.jamcollsurg.2017.11.018

[17] Lermite, E., & Arnaud, J. P. (2012). Prospective randomized study comparing quality of life after shoudice or mesh plug repair for inguinal hernia: short-term results. *Surgical technology international,* 22, 101-106. PMID: 23023573

[18] Lockhart, K., Dunn, D., Teo, S., Ng, J. Y., Dhillon, M., Teo, E., & van Driel, M. L. (2018). Mesh versus non-mesh for inguinal and femoral hernia repair. *Cochrane Database of Systematic Reviews,* 9(9), CD011517. doi: 10.1002/14651858.CD011517.pub2

[19] Lopez-Cano, M., Martin-Dominguez, L. A., Pereira, J. A., Armengol-Carrasco, M., & Garcia-Alamino, J. M. (2018). Balancing mesh-related complications and benefits in primary ventral and incisional hernia surgery. A meta-analysis and trial sequential analysis. *PLoS One*, 13(6), e0197813. doi: 10.1371/journal.pone.0197813

[20] Mohd Nurazzi, N., Asyraf, M. M., Khalina, A., Abdullah, N., Sabaruddin, F. A., Kamarudin, S. H., ... & Sapuan, S. M. (2021). Fabrication, functionalization, and application of carbon nanotube-reinforced polymer composite: An overview. *Polymers,* 13(7), 1047. doi: 10.3390/polym13071047

[21] New functional substances and materials for chemical engineering (2021). PH "Akademperiodyka", Kyiv, 2021. doi: 10.15407/akademperiodyka.444.332

[22] Sarkysov, D. S. & Perov, Yu. L. (1996). *Микроскопическая техника [Microscopic technique].* M: Медицина=M: Medicine.

[23] Plencner, M., Prosecká, E., Rampichová, M., East, B., Buzgo, M., Vysloužilová, L., ... & Amler, E. (2015). Significant improvement of biocompatibility of polypropylene mesh for incisional hernia repair by using poly-e-caprolactone nanofibers functionalized with thrombocyte-rich solution. *International journal of nanomedicine,* 10, 2635-2646. doi: 10.2147/IJN.S77816

[24] Plymale, M. A., Davenport, D. L., Walsh-Blackmore, S., Hess, J., Griffiths, W. S., Plymale, M. C., ... & Roth, J. S. (2020). Costs and complications associated with infected mesh for ventral hernia repair. *Surgical Infections,* 21(4), 344-349. doi: 10.1089/sur.2019.183

[25] Ponce Leon, F., Manso, J. E. F., Abud, V. L., Nogueira, W., Silva, P. C., & Martinez, R. (2018). Sublay repair results in superior mesh incorporation and histological fibrogenesis in comparison to onlay and primary suture in an experimental rat model. *Hernia*, 22(6), 1089-1100. doi: 10.1007/s10029-018-1808-y

[26] Qiu, W., Zhong, C., Xu, R., Zou, T., Wang, F., Fan, Y., ... & Yang, Z. (2018). Novel large-pore lightweight polypropylene mesh has better biocompatibility for rat model of hernia. *Journal of Biomedical Materials Research Part A,* 106(5), 1269-1275. doi: 10.1002/jbm.a.36326

[27] Stoikes, N., Roan, E., Webb, D., & Voeller, G. R. (2018). The Problem of Seroma After Ventral Hernia Repair. *Surgical technology international,* 32, 93-98. PMID: 29791714

[28] Tanasescu, C., Moisin, A., Mihetiu, A., Serban, D., Costache, A., & Bratu, D. G. (2021). The use of polypropylene mesh in inguinal hernia surgery: A retrospective study. *Experimental and Therapeutic Medicine,* 22(4), 1-6. doi: 10.3892/etm.2021.10627

[29] Taylor, D. (2018). The failure of polypropylene surgical mesh in vivo. *Journal of the mechanical behavior of biomedical materials*, 88, 370-376. doi: 10.1016/j.jmbbm.2018.08.041

[30] Thomas, S., Mishra, R., & Kalarikkal, N. (Eds.). (2017). *Micro and nano fibrillar composites (MFCs and NFCs) from polymer blends.* Woodhead Publishing. ISBN: 9780081019917. doi: 10.1016/B978-0-08-101991-7.09989-1

[31] Vimbela, G. V., Ngo, S. M., Fraze, C., Yang, L., & Stout, D. A. (2017). Antibacterial properties and toxicity from metallic nanomaterials. *International journal of nanomedicine*, 12, 3941-3965. doi: 10.2147/IJN.S134526

[32] Wilson, R. B., & Farooque, Y. (2022). Risks and prevention of surgical site infection after hernia mesh repair and the predictive utility of ACS-NSQIP. *Journal of Gastrointestinal Surgery,* 26(4), 950-964. doi: 10.1007/s11605-022-05248-6

ПОРІВНЯЛЬНА ОЦІНКА РЕАКЦІЇ ТКАНИН НА СІТЧАСТИЙ ІМПЛАНТАТ З ПОЛІПРОПІЛЕНУ, МОДИФІКОВАНОГО ВУГЛЕЦЕВИМИ НАНОТРУБКАМИ ТА НАНОЧАСТИНКАМИ СРІБЛА

Вільцанюк О. А., Кравченко В. М., Вільцанюк О. О., Дерезюк А. В., Шеремета Р. О.

Лікування гриж живота залишається однією з найбільш актуальних проблем сучасної хірургії. Велика кількість ускладнень після операцій з приводу гриж потребує розробки нових видів імплантатів для проведення пластики тканин. Мета дослідження - провести в експерименті порівняльну оцінку реакції тканин на імплантацію розробленого сітчастого імплантату з поліпропілену, модифікованого вуглецевими нанотрубками та наночастинками срібла. Дослідження проведені на 105

статевозрілих лабораторних щурах в трьох серіях дослідів (по 35 щурів у кожній). У першій серії в тканини передньої черевної стінки були імплантовані поліпропіленові сітчасті імплантати, в другій - поліпропіленові імплантати з покриттям антисептиком, а в третій - поліпропіленові імплантати, модифіковані вуглецевими нанотрубками та наночастинками срібла. Тварин виводили з досліду після попереднього знеболення через 3, 5, 7, 14, 21, 30 та 90 діб після операції. Вилучали тканини черевної стінки разом з імплантатами, виготовляли гістологічні препарати, які забарвлювали гематоксиліном і еозином та за Ван-Гізон. Вивчили склад і співвідношення елементів клітинної інфільтрації в тканинах з подальшою статистичною обробкою отриманих даних. Встановлено, що при імплантації сітчастих ендопротезів незалежно від їх виду на 3-5 доби після операції в тканинах виявлялися некротичні зміни з реактивним запаленням, наявність запального клітинного інфільтрату, набряк тканин та порушення мікроциркуляції. За умови імплантації розробленої сітки виявляли менш виражену ексудативну фазу запалення і більш ранній початок фази репарації. В залежності від виду використаного імплантату подальша реакція відрізнялась між групами експериментальних тварин, про що свідчили регрес явищ запалення в тканинах та процеси формування фіброзної капсули навколо імплантатів. При імплантації наномодифікованих сітчастих імплантатів до 7 доби експерименту ексудативна фаза запалення завершувалась і починалось формування тонкої сполучнотканинної капсули, формування якої завершувалось до 21 доби спостереження, тоді як при імплантації сітки з поліпропіленом та поліпропіленом з антимікробним покриттям формування капсули тривало до 30 доби. Таким чином, встановлено, що в тканинах навколо імплантації класичних сіток з поліпропілену та поліпропілену з антимікробним покриттям до 14 доби експерименту триває ексудативна фаза запалення, а сполучнотканинна капсула формується до 30 доби. В той же час, в тканинах навколо сітчастих імплантатів з поліпропілену, модифікованого вуглецевими нанотрубками та наночастинками срібла, ексудативна фаза запалення завершувалась до 7 доби експерименту. Це забезпечувало інтенсивність процесів репаративної регенерації та відмежування імплантату від навколишніх тканин тонкою сполучнотканинною капсулою до 21 доби спостереження.

Ключові слова: *поліпропіленові сітчасті імплантати, вуглецеві нанотрубки, наночастинки срібла, морфологічні зміни, біологічна сумісність.*

Author's contribution

Viltsaniuk O. A. - conceptualization, research, review writing and editing.
Kravchenco V. M. - research, methodology and writing of the original draft, formal analysis and validation.
Viltsaniuk O. O. - project administration.
Dereziuk A. V. - software, resources.
Sheremeta R. O. - data visualization.